International Journal of Rotating Machinery, 10: 55–63, 2004

ISSN: 1023-621X print
DOI: 10.1080/10236210490258070

Taylor & Francis
Taylor & Francis Group

Measurements of Strain on 310 mm Torque Converter Turbine Blades

P. O. Sweger, C. L. Anderson, and J. R. Blough
Mechanical Engineering—Engineering Mechanics, Michigan Technological University, Houghton, Michigan, USA

An automotive torque converter was tested in order to determine the effect of converter operating condition and turbine blade design on turbine blade strain in the region of the inlet core tab restraint. The converter was operated over a wide range of speed ratios (0 to 0.95) at constant input torque and a stall condition for two input torques. Foil-type strain gages in combination with wireless microwave telemetry were used to measure surface strain on the turbine blade. Strain measurements were made on two turbine blade designs.

The steady component of strain over the range of speed ratios suggests the effect of both torque loading and centrifugal loading on the turbine blade tip. The unsteady strain was greatest at stall condition and diminished as speed ratio increased. Greater input torque at stall condition resulted in both greater steady strain and greater unsteady strain. The spectral distribution of strain over the range of tested speed ratios displayed an increase in low-frequency broadband fluctuations near stall condition. A blade-periodic event is observed which correlates to the pump-blade passing-frequency relative to the turbine rotating frame. Reducing the blade-tip surface area and increasing the inlet-tab root radius reduced the range of steady strain and magnitude of unsteady strain imposed near the inlet core tab restraint over the range of operating conditions.

Keywords Blade, Microwave, Strain, Telemetry, Torque converter, Turbine, Wireless

Received 25 June 2002; accepted 1 July 2002.

This research was sponsored by GM Powertrain, a division of the General Motors Corporation. The authors wish to express their gratitude to both Ronald Buffa and Wayne Whitten of GM and Glen Barna of IR Telemetrics for technical support.

Address correspondence to P. O. Sweger, Michigan Technological University, 1400 Townsend Dr., Houghton, MI 49931. E-mail: posweger@mtu.edu

The automotive torque converter transfers rotational energy from an engine to a transmission through a viscous and incompressible working fluid. The three primary elements of a converter are the pump, turbine and stator. Each element is composed of a number of blades shaped such that they redirect the flow of oil passing though them, resulting in a change in angular momentum of the working fluid. While the converter is designed to perform optimally at a particular condition, it must function satisfactorily over a diverse range of conditions including idle, stall, near couple, and overspeed.

Several previous studies have been conducted to better understand the nature of oil flow within the torque converter, with the primary concern being converter efficiency and performance. Dong et al. (1998) used a miniature high-frequency-response five-hole probe to find that the flow pattern at the pump exit is complex. The flow structure was described as having four main regions: the free-steam, the pump blade wake, the core-suction corner separation, and the intense mixing region. Additionally, a strong secondary flow was observed along with unsteadiness dominated by the pump blade passing frequency. Brun and Flack (1997a) used laser velocimetry to demonstrate a strong jet-wake region which propagates across the turbine inlet plane at the pump-turbine interaction frequency. Throughflow velocity unsteadiness and incidence angle unsteadiness, due to pump-turbine blade interaction, was found to be greater at a high speed-ratio (SR = 0.8) compared to near-stall (SR = 0.065). This is possible when the flow enters the turbine at approximately 45° from the normal plane in the high speed ratio condition where as the flow enters the turbine more obliquely for the stall condition, approximately 72° from the normal plane. Since the relative inlet flow angle was larger at the near-stall condition this suggests larger cyclic forces being imposed on the turbine blades. This is consistent with Liu (2001) who found total unsteady static pressure measurements on the turbine shell at the 12% chord length to be much greater near stall (SR = 0.065) than at high speed ratio (SR = 0.6 or 0.8). Liu attributes this to the large incidence angle and corresponding strong flow mixing at low speed ratio. While there is a significant body of literature that examines the

flow field within the torque converter, there is little found on fluid-blade interaction.

Micro-cracks have been observed in the turbine blades of a 310 mm torque converter after severe-duty testing conditions. The cracks originate at the small radius of the inlet-tab pressure-side and propagate across the blades' width and thickness. The crack runs parallel with the line of bending of the unrestrained blade-tip and has the appearance of a transgranular brittle failure. These observations are consistent with what is described as a fatigue failure by Higdon et al. (1985). As the design of the torque converter tends toward flatter aspect ratios, the fluid motion may further aggravate blade loading and cracking. Ejiri and Kubo (1999) found that measured efficiency and torque capacity deteriorate with flatter designs. Corresponding numerical analysis indicated that a more pronounced jet-wake flow occurs at the pump exit with the flatter converter design, while efficiency loss at the pump inlet is attributed to an increased shock loss.

No *in situ* strain measurements have been reported for the turbine of a torque converter. Experimental measurements within a converter are complicated by the fact that the converter is a sealed, pressurized, and rotating vessel which houses the independently rotating turbine. Wireless microwave telemetry has been used successfully in a number of measurement applications (Cross, 1998; Zeng, 2000), and is well suited for the measurement of strain on the converter turbine blade.

The objective of this work was two-fold: 1) correlate strain measurements with converter operating condition and the underlying fluid dynamics, and 2) substantiate expected improvements in strain level with blade design changes.

METHODS

Experimental Converter

An important performance parameter in converter design and testing is the input K factor, a semi-dimensionless number which describes the relationship between pump torque and pump speed for a given converter design. Changes in performance characteristics are accomplished by altering the angle and shape of blade elements, most significantly with the pump exit angle. A single value for K factor (measured at stall condition) is generally utilized in comparing converters of different design, and can be used as a model designation for a particular set of blade elements.

Three 310 mm torque converter assemblies were tested: 87, 101, and 117 K factor. The selected K factors were accomplished by various combinations of pump and stator with a common turbine and cover, as detailed in Table 1. The pumps and cover were fabricated with a bolt-together flange so that internal parts could be interchanged.

A special 36-blade turbine was built for the purposes of this investigation. One-half of the turbine blades were of a conventional design (blade A) while the other half were modified (blade B) with the intention of reducing strain levels. Turbine blade B is distinguished by a larger tab-root radius, and reduced tip length, as shown in Figure 1. Both blade designs were of 1.14 mm nominal thickness. The turbine blades were installed as 4 groups, alternating 9 blades of each design.

TABLE 1
Torque Converter Component Description

Converter K factor	87	101	117
Pump blades	29	29	29
Inlet angle, degrees	−30	−30	−30
Exit angle, degrees	30	30	10
Turbine blades	36	36	36
Inlet angle, degrees	61	61	61
Exit angle, degrees	−63	−63	−63
Stator blades	19	14	14
Inlet angle, degrees	21	40	40
Exit angle, degrees	58	63	63

Three turbine blades were affixed with foil-type strain gages. Each instrumented blade received a strain gage half-bridge on both the pressure and suction side, directly opposite to one another. A half-bridge consisted of an active gage located in the vicinity of the inlet core-tab and a zero-strain reference gage located on the blade tab-surface inside the torus core. Two blades, one blade A and one blade B, received a single-direction strain gage oriented to respond to strain in the direction of oil flow, relative to turbine passage. A third blade, blade B design, received a three-gage rosette oriented to respond to strain in the direction of hydraulic oil flow, 45° to the flow, and perpendicular to the flow. During instrumentation it was found that the strain rosette of blade B pressure side could not be balanced

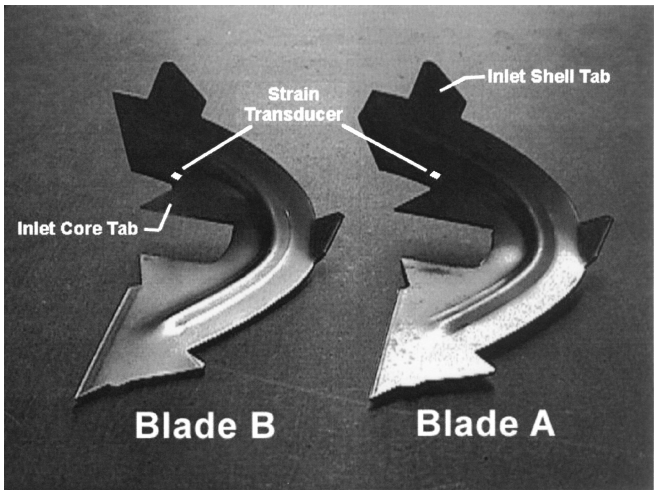

FIGURE 1
Conventional (A) and modified (B) converter turbine blades. Cracks observed in blade A during dynamometer endurance testing, beginning at the inlet core-tab on the pressure surface and propagating across to the inlet shell-tab.

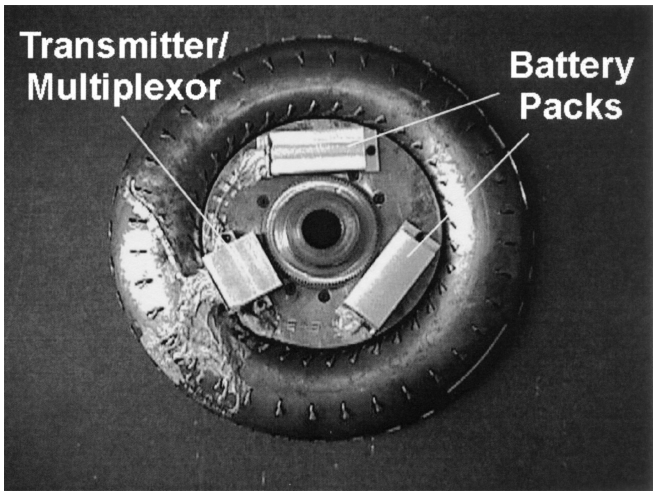

FIGURE 2
Microwave telemetry assembly installed on 310 mm converter turbine. Note: The clutch plate has been removed.

in the usable range and were therefore not used in this investigation. Results from the remaining rosette transducer are not presented as a comparison between blades A and B was not available.

Wireless microwave telemetry was used to transmit strain-transducer signals out of the converter. The telemetry transmitter was installed on the turbine in place of the converter clutch plate and consisted of battery packs, a multiplexor and the microwave transmitter, as shown in Figure 2. The transmitter was capable of time-sequence multiplexing seven transducer signals to be transmitted from the turbine through antenna slots in the converter cover to the reception antenna located in the converter test fixture. The operation of the microwave telemetry is described by Cross (1998) and Zeng (2000). Each transducer signal was transmitted for 0.5 seconds in turn before the sequence was repeated. A marker signal following the seventh channel provided a reference to identify the various strain transducers. A microwave receiver transformed the frequency-modulated microwave signal to an analog voltage, followed by 2,000 Hz low-pass filtering.

The installation of a microwave telemetry instrument has the potential of disturbing the proper operation of the torque converter. Production build specifications require rotational unbalance of less than 12 g-cm in the turbine element. After telemetry instrumentation the turbine was balanced to 1.1 g-cm. The converter cover was also modified with the addition of six 1 mm wide slots to allow the microwave signal to be re-radiated. Each slot was sealed with an ultra-gray RTV, which was pressure tested at operating conditions prior to the experimental tests.

Microwave signal emitted from the torque converter can reflect off the interior surfaces of the converter test fixture thus creating interference regions. The signal reception was enhanced by partially lining the test fixture with microwave absorbing foam.

Data Processing

The analog voltage signal was digitized at 5,000 samples/second. Five seconds of strain data were captured for each test condition to ensure a complete sweep of all multiplexed channels. Acquisition was initiated by a trigger signal from the dynamometer controller indicating steady-state converter operation. Strain data was recorded to electronic media along with signals for pump speed, turbine speed, pump torque, and turbine torque.

The multiplexed data was separated into individual records according to strain gage. Each record was 2,048 samples (approximately 0.41 seconds) to provide adequate data for mean and root-mean-square calculations, and to facilitate transformation to the frequency domain.

The instantaneous strain measured at any particular time is the result of an unsteady component of strain superimposed on a steady component of strain. Mathematically, the strain can be expressed as:

$$\varepsilon = \bar{\varepsilon} + \varepsilon' \quad [1]$$

The steady strain is represented by the time-averaged value of measured strain and is determined from:

$$\bar{\varepsilon} = 1/n \, \Sigma i = 1 \text{ to } n, \varepsilon_i \quad [2]$$

The unsteady strain reflects perturbations about the steady strain value and is characterized using a root-mean-square (rms) value:

$$\varepsilon' = (1/n \, \Sigma i = 1 \text{ to } n, (\varepsilon_i - \bar{\varepsilon})^2)^{1/2} \quad [3]$$

Microstrain was determined from the change in transducer signal relative to a reference value and a calibration constant. The following expression was used in calculating the instantaneous strain:

$$\varepsilon = B \cdot (V - V_o) \quad [4]$$

The transducer bridges were found to have temperature dependence despite the use of a compensating transducer mounted on a strain-free surface of the turbine blade. Since both V and V_o were dependent on temperature, the following general expression was used to correct both the test voltage and the reference voltage:

$$V_{\text{corr}} = V_{\text{meas}} - m \cdot (T - T_{\text{ref}}) \quad [5]$$

A reference temperature (T_{ref}) of 93°C was selected, as it was the typical temperature observed at the initiation of a test. All temperature measurements were made on the oil flow exiting the torque converter fixture. Although zero-strain was measured while the oil was still hot, the temperature was not recorded at this condition. Consequently, no compensation for changes in temperature between zero conditions could be made. Hence, values of steady strain are reported relative to the selected reference

temperature and not an absolute scale. The measurement uncertainty for steady strain was plus or minus 35 uS (95% confidence interval), while the measurement uncertainty for unsteady strain was on the order of the data acquisitions resolution capabilities, plus or minus 1.5 uS.

The turbine blade-tip is presumed to behave as a cantilever beam where the surface strain at identical locations on opposite surfaces of the blade will experience equal, yet opposite, magnitudes of strain. This assumption may not be perfect due to curvature in the turbine blade and other geometric non-uniformities, nevertheless the measured strain of opposing strain-transducers was averaged together for a mean-blade response. Strain results appear well behaved when considered as a mean-blade response. The sense of strain (tension versus compression) of the pressure-side strain was reversed before averaging with the suction-side strain, and hence steady strain values reflect suction-side measures. The unsteady strain did not require the sense of strain to be reversed, as the values are inherently positive.

Spectral distribution of unsteady strain was calculated by a fast fourier transform on the time domain data. The sample size was reduced to a power of two (2,048 samples) to facilitate the transformation to frequency domain and a Hanning window was used on the data with an appropriate correction factor. The steady component (0 Hz) of the spectral distribution was removed for graphical presentation purposes. Spectral amplitudes were calculated at frequency increments of 2.44 Hz.

Test Conditions

Turbine blade strain was measured for a variety of operating conditions. These included a 300 Nm efficiency test, 300 Nm stall test, and 200 Nm stall test. Each test was performed three times to evaluate repeatability. The efficiency test consisted of a sweep through turbine speeds from 200 to 3,000 RPM in 200 RPM steps while pump torque was maintained at 300 Nm. This range of turbine speeds ensured that the coupling point ($T_t = T_p$) was achieved. An overspeed condition ($n_t = 3{,}200$ RPM and $n_p = 2{,}500$ RPM) was included as part of the efficiency test following the sweep of turbine speeds. Unfortunately, no torque was measured at the overspeed condition due to calibration limits and the strain results for this condition are not presented. The stall test consisted of operating the torque converter at either 200 or 300 Nm pump torque while the turbine speed was maintained at zero RPM. The 117 K factor converter was not tested at 300 Nm stall condition due to an excessive rise in hydraulic oil temperature across the converter.

All torque converter testing was performed in a laboratory test fixture with pump and turbine loads provided by dynamometer. Each test point was maintained at steady state for 7 seconds while data was collected. Additional strain data was collected before and after each test sequence to provide a zero-strain correction, despite not measuring temperature at this condition. During zero strain measurements, hydraulic oil circulated through the converter yet the converter did not rotate. During testing, a cool down sequence was initiated if the hydraulic oil temperature reached 120°C in order to protect the telemetry instrument from thermal damage.

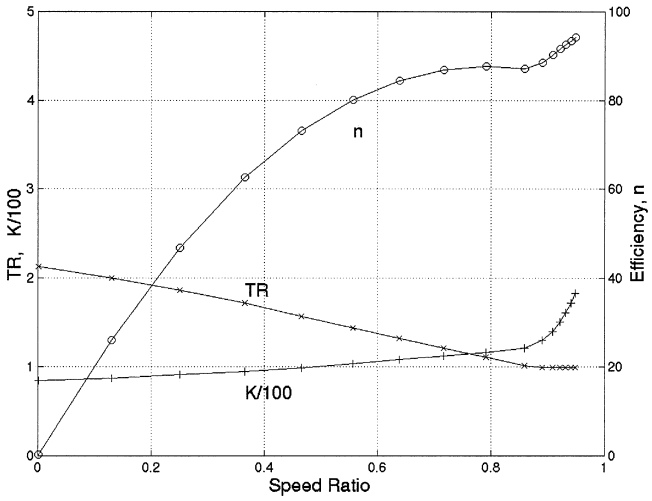

FIGURE 3
Dimensionless performance characteristics of 310 mm 87 K torque converter for 300 Nm efficiency and stall test.

Converter Performance

Dimensionless performance characteristics of the 87 K factor converter for steady-state operation are shown in Figure 3. Here, the coupling point (lowest SR where TR = 1) is observed to occur at approximately a speed ratio of 0.9. Dynamometer performance was extremely consistent over the three repetitions of each test condition, never exceeding 0.35% of standard error.

RESULTS AND DISCUSSION

The steady strain results for the 87 K factor converter are shown in Figure 4 (300 Nm efficiency test) and Figure 6 (300 and 200 Nm stall test) while the unsteady strain results are shown in Figure 7 (300 Nm efficiency test) and Figure 8 (300 and 200 Nm stall test). A spectral distribution of the unsteady strain results for the 87 K factor converter are shown in Figure 9. Results for the 101 and 117 K factor converters are not presented as the trends observed are not materially different from the 87 K factor converter.

Steady Strain

The effect of speed ratio on steady strain is shown in Figure 4. The suction-side of the turbine blade becomes less compressive as the speed ratio increases from stall condition (SR = 0) up to the coupling point (SR = 0.9). Changes in suction-surface compression over this range of speed ratios is primarily the result of a reduction in fluid incidence with the blade-tip pressure-surface. By and Lakshminarayana (1995) explain observations in static pressure distribution in the turbine by the greater throughflow velocity and fluid-turning which occurs at stall condition. Brun

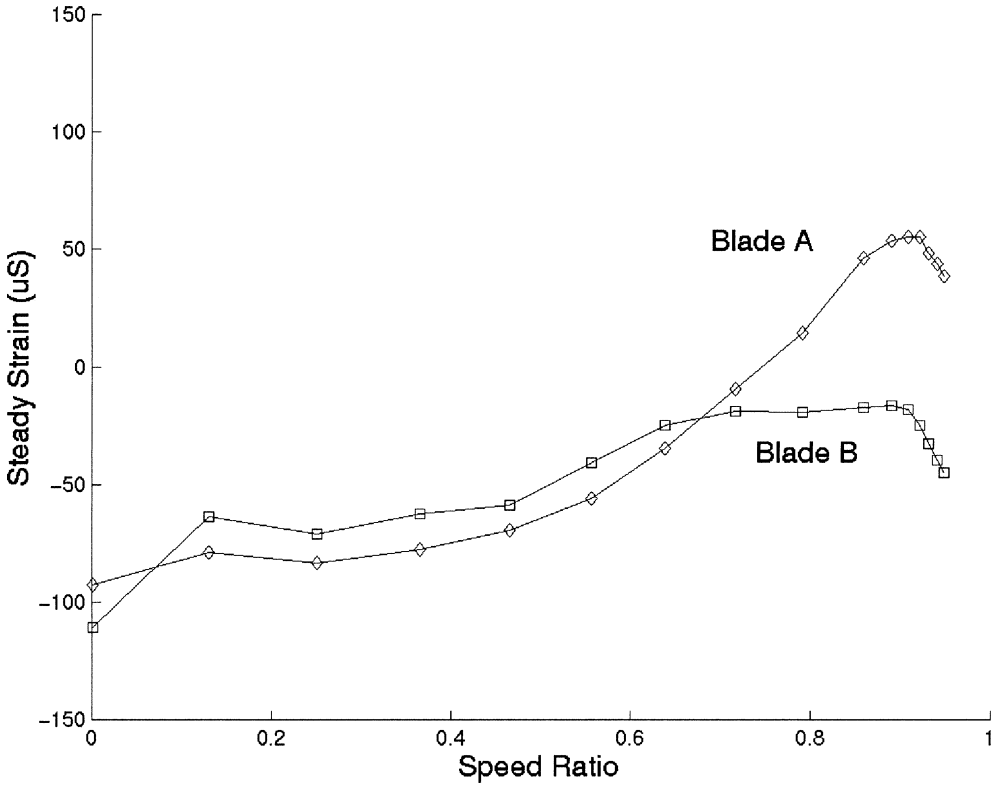

FIGURE 4

Steady strain measured on two blade designs of 310 mm 87 K torque converter for 300 Nm efficiency and stall test. Strain represents that of the suction surface of turbine blade, where negative (−) indicates compression. Note: Steady strain does not represent an absolute scale.

and Flack (1997b) showed that the oil mass flow decreases 32% as speed ratio increases (from SR = 0.065 to 0.8) while the angle of fluid incidence with the turbine blade-tip changes from 26.8° (impacting the pressure-side) to negative 5.8° (impacting the suction-side). The suction surface becomes the least compressive at a speed ratio of 0.9. Turbine blade B experienced a smaller change in steady strain (95 uS) over the range of operating conditions than did blade A (148 uS). Blade B offers a smaller surface area for the incident fluid to act on as well as providing a shorter distance for the bending moment between the center of pressure and the line of cracking. Additionally, the larger tab-root radius of blade B reduces the stress concentration at the location of strain measurement.

At speed ratios above 0.9 a tendency towards compression is shown in Figure 4. This trend with increasing speed ratio is primarily the result of centrifugal loading on the turbine blade-tip. The orientation of the turbine blade-tip is such that the suction-surface will become compressive as the tip bends radially outward with centrifugal loading. Figure 5A depicts the normal (radially outward) acceleration experienced at the inlet of the turbine for the range of speed ratios tested. Figure 5B shows an estimate of the component of fluid velocity incident

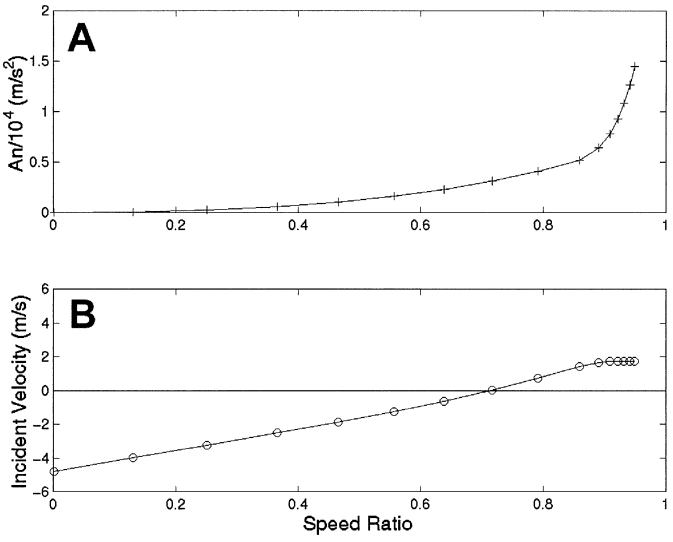

FIGURE 5

Calculated radial acceleration (A) and estimated oil velocity component incident (B) at the turbine blade tip of a 310 mm 87 K torque converter for 300 Nm efficiency and stall test.

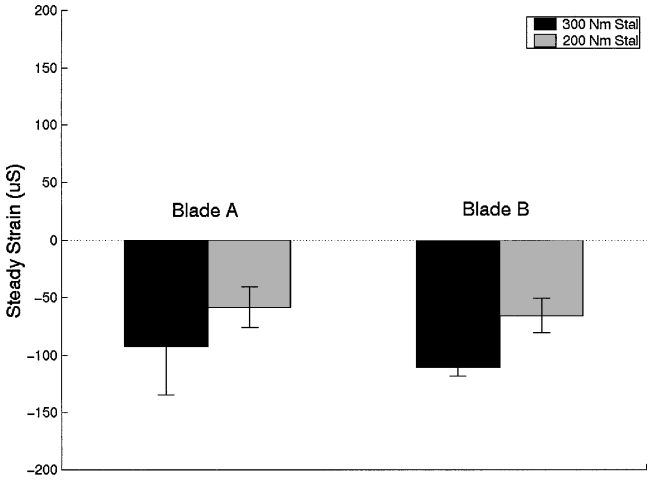

FIGURE 6
Steady strain measured on two blade designs from a 310 mm torque converter for 300 Nm and 200 Nm stall test ($n_t = 0$). Error bars indicate standard deviation.

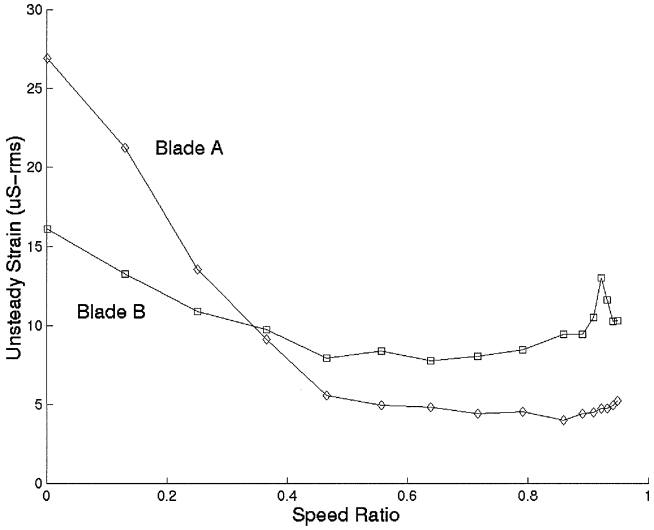

FIGURE 7
Unsteady strain measured on two blade designs from a 310 mm 87 K torque converter for 300 Nm efficiency and stall test.

on the blade surface, calculated from one dimensional analysis. It appears that turbine blade-tip steady strain is dominated by fluid incidence at low speed ratios while centrifugal effects overcome the incidence of fluid on the suction surface for high speed ratios.

The effect of pump torque on steady strain at stall condition (SR = 0) is shown in Figure 6. The 300 Nm stall test produced more steady strain than that of the 200 Nm as a result of both increased mass throughflow and increased pump speed. At stall condition the pump speed increases with pump torque according to the relationship $n_p = K(T_p)^{1/2}$. As the pump rotational speed increases the fluid exiting the pump will have a greater tangential velocity component. Furthermore, one-dimensional analysis indicates 22% higher mass throughflow rates for the greater pump torque condition, with the associated higher relative velocity of fluid exiting the pump. The combined effect of increased mass throughflow and increased pump speed results in a greater absolute fluid velocity delivered to the turbine inlet. At stall condition the fluid impacts the turbine blade tip on the pressure surface with a large angle of incidence (the angle of incidence between the 200 Nm and 300 Nm stall conditions is relatively constant). The higher fluid velocity of the 300 Nm condition experiences a larger change in momentum which requires a larger reaction force from the turbine blade tip leading to more compressive steady strain on the suction surface.

A direct comparison between blade A and blade B, for a given operating condition, can not be made due to the possible effects of turbine thrust load, calibration issues and temperature dependency.

Unsteady Strain

The unsteady component of the instantaneous strain was calculated as the rms-fluctuations about the time-averaged value, and is shown as a function of speed ratio in Figure 7. The predominant characteristic of unsteady strain is the maximum value at stall condition which rapidly decreases as speed ratio approaches 0.5. As suggested by Brun and Flack (1997a) there are larger cyclic forces imposed on the turbine blade near stall condition. The larger incidence angle of fluid flow with respect to the turbine blade at stall condition is the dominant influence, inducing more severe blade-tip bending. Fluctuations in fluid velocity at the turbine inlet are the result of the upstream pump blade wake causing a non-uniform flow field.

The unsteady strain remains relatively constant (5–10 uS-rms) for speed ratios between 0.5 and 0.8. This magnitude of unsteady strain is on the order of the inherent noise observed while measuring strain at the zero reference condition. It would seem that the unsteady strain for this range of speed ratios is no different than while the converter sits idle. Conclusions regarding the difference in unsteady strain over this range of operating conditions cannot be made at this time.

Unsteady strain increases slightly as speed ratio increases above 0.8 and is most likely the result of fluctuations in fluid velocity incident with the suction surface, as indicated by Figure 5B. It is unclear why blade B experiences a sudden peak in unsteady strain at a speed ratio of 0.92 while blade A shows no similar behavior for identical operating conditions. This will be the subject of a future investigation.

The effect of pump torque on unsteady strain at stall condition is shown in Figure 8. The unsteady strain resulting from the 300 Nm stall is consistently greater than during the 200 Nm stall. While one-dimensional analysis indicates that the mean throughflow rate is greater while the incident angle remains constant for greater pump torque at turbine stall, it fails to indicate how the velocity fluctuations change. It is hypothesized that fluctuations in throughflow velocity resulting from the upstream pump blade wake are greater for the higher pump torque at stall condition.

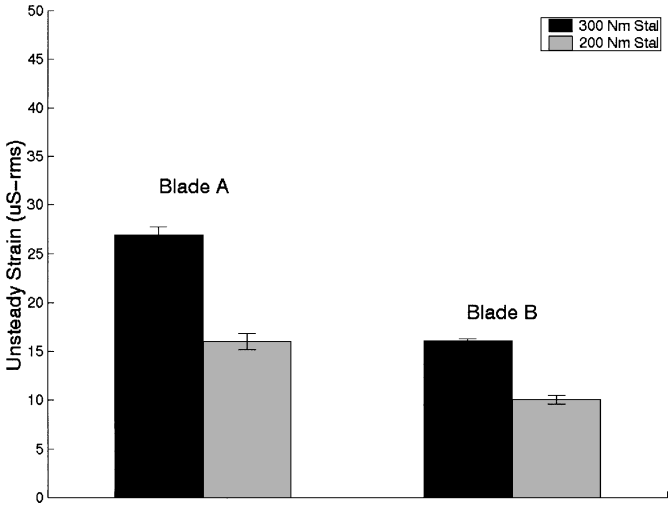

FIGURE 8
Unsteady strain measured on two blade designs from a 310 mm 87 K torque converter at stall condition ($n_t = 0$) for 300 Nm and 200 Nm. Error bars indicate standard deviation.

Blade B experienced less unsteady strain than blade A for identical operating conditions. The smaller surface area and shorter distance between center of pressure and line of bending explains why blade B is less sensitive to fluid velocity fluctuations.

Spectral Distribution of Unsteady Strain

The effect of speed ratio on the spectral distribution of strain is shown in Figure 9. The suction surface strain-data for both blade A and B are included. The waterfall plots indicate strain intensity as a function of spectral distribution and speed ratio, where high intensity is represented by red and low intensity by blue. The greatest strain intensity is observed at low speed ratios, predominantly over the 0–1000 Hz range. This demonstrates that the greater value of unsteady strain at stall condition, shown in Figure 7, is the result of broadband fluctuations over this frequency range. The variation of strain-intensity with speed ratio is more apparent in blade A than blade B, further supporting the notion that blade B is less sensitive to unsteady fluid effects. Blade B shows a minor increase in strain intensity at the highest speed ratio, predominately in the lower frequency range. This demonstrates that the small rise in unsteady strain shown in Figure 7 at high speed ratios is also a result of broadband fluctuations over the low frequencies, similar to that observed at stall condition.

A distinct line of high strain intensity which is linearly related to speed ratio is visible in the waterfall plot of Figure 9. The frequency of this high intensity strain is a multiple of 29 times the relative pump-to-turbine rotational speed, identifying it as a pump blade passing frequency, as there are 29 pump blades in the converter assembly. Marathe et al. (1997) were able to identify various harmonics of turbine speed, turbine blade passing,

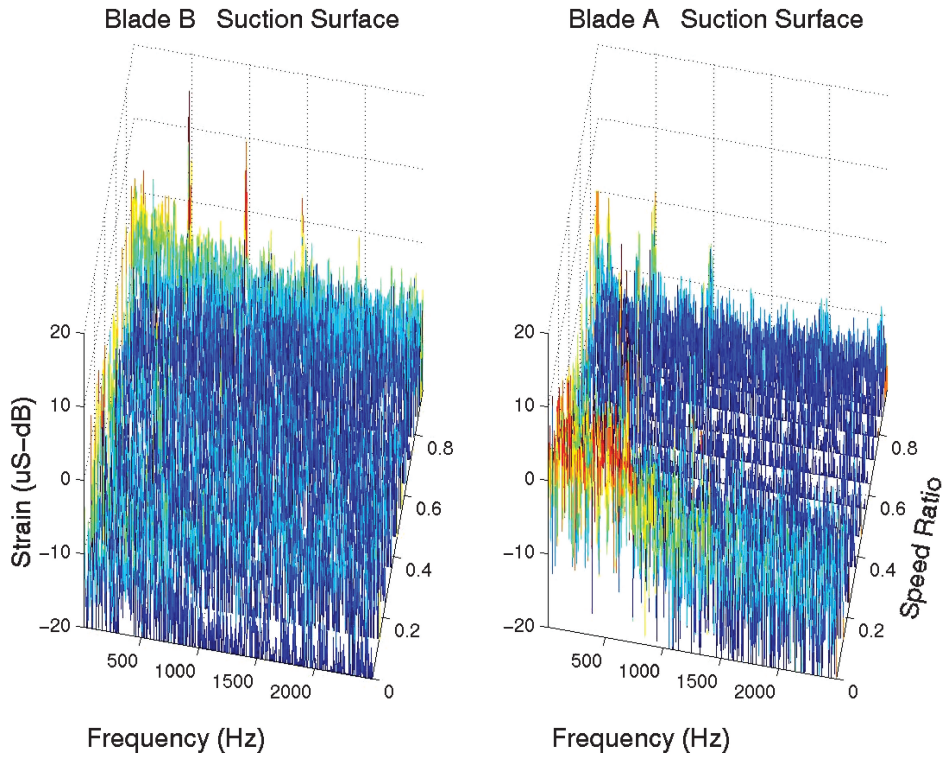

FIGURE 9
Spectral distribution of unsteady strain for: (A) blade A, and (B) blade B; measured on 310 mm 87 K torque converter for 300 Nm efficiency and stall test.

and relative pump blade-to-turbine frequencies in static pressure measurements on the stator surface. Dong et al. (1998) identified the first seven harmonics of the pump-blade passing frequency in the total pressure measurements at the pump exit. These fluctuations in total pressure were dissipated at the exit of the turbine. Finally, Dong and Lakshminarayana (2001) were able to show that stator-passage passing frequencies visible in the pressure fluctuations at the pump mid-chord are dissipated by the pump exit. While at the same time a relative turbine blade-to-pump passing frequency became visible at the pump exit.

Blade B has a uniformly higher strain intensity for speed ratios greater than zero, compared to blade A. This reveals that the greater unsteady strain of blade B in Figure 7 is the result of a uniformly greater strain intensity over the entire frequency range. Because this magnitude of unsteady strain is within the level of inherent noise of the measurement system, it is possible that greater strain intensity, indicated in Figure 9, is immaterial to the behavior of the turbine blades.

Two peaks in strain intensity, at approximately 493 and 985 Hz, are observed at a number of measurement locations throughout the testing conditions. These peaks are not fully understood but appear to originate in the receiver of the wireless telemetry system and are subject to further investigation. However, filtering these frequencies from the data demonstrates that they do not materially affect the results presented herein.

SUMMARY AND CONCLUSIONS

Foil-type strain gages were used in conjunction with wireless microwave telemetry to make *in-situ* measurements of turbine blade-tip strain in an 87 K factor torque converter for two blade designs over a range of speed ratios and at two pump torques during stall condition. Time-averaged, root-mean-square, and spectral distribution of strain results are presented and discussed. The following conclusions are drawn from this investigation:

1. Turbine blade-tip steady strain is dominated by fluid incidence at low speed ratios (SR = 0–0.6) while centrifugal effects overcome the incidence of fluid on the suction surface at high speed ratios (SR > 0.9).
2. Turbine blade-tip unsteady strain is most severe at stall condition due to the combined effect of large pressure-side fluid incidence angle relative to the turbine blade and throughflow velocity fluctuations. The unsteady strain diminishes rapidly with increasing speed ratio as a result of decreasing fluid incidence angle with the blade surface.
3. Turbine blade-tip fluctuations are primarily composed of low-frequency broadband (0–1000 Hz) fluctuations at stall condition, which decrease at higher speed ratios.
4. A strong periodic pump-blade passing event is evident in the frequency domain of turbine blade-tip fluctuations throughout the range of operating conditions.
5. Reducing the blade-tip surface area and increasing the inlet-tab root radius reduced the range of steady strain and magnitude of unsteady strain imposed near the inlet core tab restraint over the range of operating conditions.

NOMENCLATURE

A_n	normal acceleration (ω^2/r), m/s^2
B, m	calibration constant
i	record index
K	input K factor ($n_p/T_p^{1/2}$)
n	record length
n_t	turbine speed, RPM
n_p	pump speed, RPM
r	radius, m
rms	root mean square
SR	speed ratio (n_t/n_p)
T	temperature, °C
T_{ref}	reference temperature, °C
T_t	turbine torque, Nm
T_p	pump torque, Nm
TR	torque ratio (T_t/T_p)
V	strain signal voltage, volts
V_o	zero-strain voltage, volts
V_{meas}	non-temperature compensated, volts
V_{corr}	temperature compensated, volts
ε	instantaneous strain, in/in
$\bar{\varepsilon}$	steady strain, in/in
ε'	unsteady strain, in/in-rms
η	power efficiency (SR * TR)
ω	angular speed, rad/s

REFERENCES

Brun, K., and Flack, R. D. 1997a. Laser velocimeter measurements in the turbine of an automotive torque converter: Part II, Unsteady measurements. *ASME Journal of Turbomachinery* 119:655–662.

Brun, K., and Flack, R. D. 1997b. Laser velocimeter measurements in the turbine of an automotive torque converter, Part I, Steady measurements, *ASME Journal of Turbomachinery* 119:646–654.

By, R. R., and Lakshminarayana, B. 1995. Measurement and analysis of static pressure field in a torque converter turbine. *ASME Journal of Fluids Engineering* 117:473–478.

Cross, T. 1998. Cavitation signatures in an automatic transmission torque converter. M.S. Thesis, Michigan Technological University.

Dong, Y., Lakshminarayana, B., and Maddock, D. 1998. Steady and unsteady flow field at pump and turbine exits of a torque converter. *ASME Journal of Fluids Engineering* 120:538–548.

Dong, Y., and Lakshminarayana, B. 2001. Rotating probe measurements of the pump passage flow field in an automotive torque converter. *ASME Journal of Fluids Engineering* 123:81–91.

Ejiri, E., and Kubo, M. 1999. Influence of the flatness ratio of an automotive torque converter on hydrodynamic performance. *ASME Journal of Fluids Engineering* 121:614–620.

Higdon, A., Ohlsen, E. H., Stiles, W. B., Weese, J. A., and Riley, W. F. 1985. Mechanics of Materials, 4th ed., New York: John Wiley & Sons.

Liu, Y. F. 2001. An experimental investigation of fluid dynamics and performance of an automotive torque converter. Ph.D. Dissertation, The Pennsylvania State University, University Park.

Marathe, B. V., Lakshminarayana, B., and Maddock, D. 1997. Experimental investigation of steady and unsteady flow field downstream of an automotive torque converter turbine and inside the stator, Part II: Unsteady pressure on the stator blade surface. *ASME Journal of Turbomachinery* 119:634–645.

Zeng, L. 2000. Experimental investigation of cavitation signature in an automotive torque converter. M.S. Thesis, Michigan Technological University.